



## Thermal Conductance of a Single-Electron Transistor

B. Dutta,<sup>1</sup> J. T. Peltonen,<sup>2</sup> D. S. Antonenko,<sup>3,4,5</sup> M. Meschke,<sup>2</sup> M. A. Skvortsov,<sup>3,4,5</sup> B. Kubala,<sup>6</sup>  
J. König,<sup>7</sup> C. B. Winkelmann,<sup>1</sup> H. Courtois,<sup>1</sup> and J. P. Pekola<sup>2</sup>

<sup>1</sup>*Université Grenoble Alpes, CNRS, Institut Néel, 25 Avenue des Martyrs, 38042 Grenoble, France*

<sup>2</sup>*Low Temperature Laboratory, Department of Applied Physics, Aalto University School of Science, P.O. Box 13500, 00076 Aalto, Finland*

<sup>3</sup>*Skolkovo Institute of Science and Technology, Skolkovo, 143026 Moscow, Russia*

<sup>4</sup>*L. D. Landau Institute for Theoretical Physics, 142432 Chernogolovka, Russia*

<sup>5</sup>*Moscow Institute of Physics and Technology, Moscow, 141700, Russia*

<sup>6</sup>*Institute for Complex Quantum Systems and IQST, University of Ulm, 89069 Ulm, Germany*

<sup>7</sup>*Theoretische Physik and CENIDE, Universität Duisburg-Essen, 47048 Duisburg, Germany*

(Received 11 April 2017; published 15 August 2017)

We report on combined measurements of heat and charge transport through a single-electron transistor. The device acts as a heat switch actuated by the voltage applied on the gate. The Wiedemann-Franz law for the ratio of heat and charge conductances is found to be systematically violated away from the charge degeneracy points. The observed deviation agrees well with the theoretical expectation. With a large temperature drop between the source and drain, the heat current away from degeneracy deviates from the standard quadratic dependence in the two temperatures.

DOI: [10.1103/PhysRevLett.119.077701](https://doi.org/10.1103/PhysRevLett.119.077701)

The flow of heat at the microscopic level is a fundamentally important issue, in particular, if it can be converted into free energy via thermoelectric effects [1]. The ability of most conductors to sustain heat flow is linked to the electrical conductance  $\sigma$  via the Wiedemann-Franz law:  $\kappa/\sigma = L_0 T$ , where  $\kappa$  is the heat conductance,  $L_0 = \pi^2 k_B^2 / 3e^2$  the Lorenz number, and  $T$  the temperature. While the understanding of quantum charge transport in nano-electronic devices has reached a great level of maturity, heat transport experiments are lagging far behind [2], for two essential reasons: (i) Unlike charge, heat is not conserved, and (ii) there is no simple thermal equivalent to the ammeter. Heat transport can nevertheless give insight to phenomena that charge transport is blind to [3,4], and, remarkably, a series of experiments has demonstrated the very universality of the quantization of heat conductance, regardless of the carriers' statistics [3–11].

As device dimensions are reduced, electron interactions gain capital importance, leading to Coulomb blockade in mesoscopic devices in which a small island is connected by tunnel junctions. A metallic island connected to a source and a drain through tunnel junctions exceeding the Klitzing resistance  $R_K = h/e^2$  and under the influence of a gate electric field constitutes a single-electron transistor (SET) [12]. The charging energy of the island by a single electron is written  $E_C = e^2/2C$ , where  $C$  is the total capacitance of the island. It defines the temperature and bias thresholds below which single-electron physics appears. In the regime where charge transport is governed by unscreened Coulomb interactions, the question of the associated heat flow has been addressed by several theoretical studies

[13–20]. The Wiedemann-Franz law is expected to hold in an SET only at the charge degeneracy points in the limit of small transparency, where the effective transport channel is free from interactions, and is violated otherwise.

In this Letter, we report on the measurements of both the heat and charge conduction through a metallic SET, with both quantities displaying a marked gate modulation. A strong deviation from the Wiedemann-Franz law is observed when the transport through the SET is driven by the Coulomb blockade, as the electrons flowing through the device are then filtered based on their energy.

Figure 1(a) is a colored scanning electron micrograph of one of the devices that we have investigated, while Fig. 1(b) shows a schematic with the same colors for every element. It includes an SET with a drain made of a bulky electrode that is well thermalized to the bath. In contrast, the source of the SET is connected to its lead through a direct normal-metal–superconductor ( $N$ - $S$ ) contact, which thermally isolates it due to poor thermal conductivity of a superconductor at a low temperature. In addition, four superconducting contacts form superconductor–insulator–normal-metal ( $S$ - $I$ - $N$ ) junctions. As will be discussed below, the latter can be used either as electronic thermometers or coolers (or heaters). Samples were fabricated by three-angle evaporation of Cu (30–45 nm), Al (20 nm), and again Cu (30 nm) [21]. The Al layer was oxidized in order to form tunnel barriers with the second Cu layer. Still, the drain, island, and source are in the normal state, as the SET tunnel junctions are based on a short Al strip rendered normal by the inverse proximity effect via a clean contact to a long normal (Cu) line [30]. The SET island was designed

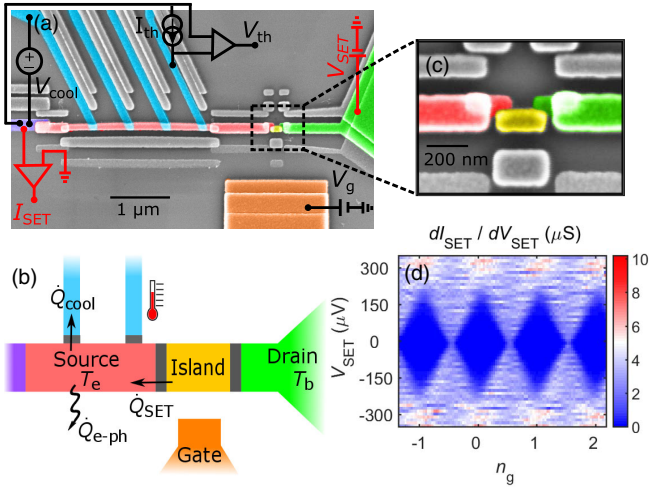


FIG. 1. A single-electron transistor and the setup for the heat transport measurement. (a) False-colored SEM image of the full device. The circuit in red indicates the charge transport setup, while the black one stands for the heat transport setup. (b) Schematic of the device, with the different elements shown in colors. (c) Enlarged view of the central part of the SET. (d) Differential conductance map of the sample A SET at 50 mK against drain-source voltage  $V_{\text{SET}}$  and induced charge  $n_g$ .

with a small volume in order to render the electron-phonon coupling negligible in the island.

We report here on two investigated devices with nearly identical geometry but different drain-source tunnel resistance  $R_N$  of 164 (sample A) and 52 k $\Omega$  (sample B). Figure 1(d) shows the differential conductance at 50 mK as a function of both the SET bias  $V_{\text{SET}}$  and the average number  $n_g = C_g V_g / e$  of electrons induced electrostatically by the gate potential  $V_g$  on the island. Here  $C_g$  is the capacitance between the gate and the island. Coulomb diamonds (in dark blue) are regions of zero current through the SET. Every diamond is centered around an integer value of  $n_g$  and defines a fixed charge state on the island. At zero bias, the charge conductance is thus vanishing, except in the vicinity of the degeneracy points at half-integer values of  $n_g$ . At these points, two charge states have the same energy, and the conductance (for small barrier transparency) is half the high-temperature value, which is related to the fact that only these two states are involved. From the map, one can estimate a charging energy  $E_C$  of about 155 and 100  $\mu\text{eV}$  for sample A and B, respectively.

In the present work, our approach is to study the thermal balance in the source when it is heated or cooled. In every thermal measurement, we ensured that no current is flowing through the SET, so that pure heat transport can be considered. The thermal conductance of the SET is inferred from the heat balance in the source and then compared to the electrical conductance measured in parallel.

We will consider here that the electron population of the source is in quasiequilibrium at a well-defined (electronic)

temperature  $T_e$ . This is justified, as the mean electron escape time from this element is longer than the estimated electron-electron interaction time [31]. By heating or cooling electrons in the source, its electronic temperature  $T_e$  can be different from the temperature of the phonons thermalized at the bath temperature  $T_b$ . We achieve electronic thermometry by measuring the voltage drop across a current-biased  $N$ - $I$ - $S$  junction [32,33], the current set point being chosen to be low enough in the subgap regime ( $eV < \Delta$ ,  $\Delta$  being the energy gap of the superconductor) to avoid any significant cooling.

Indeed, a current bias through a (pair of)  $N$ - $I$ - $S$  junctions enables one to cool electrons with respect to the phonons [34]. This can be understood as a kind of selective evaporation: When the voltage drop is below the energy gap, only higher energy electrons can escape the normal metal. The maximum cooling power is obtained right below the gap in terms of the voltage drop across one  $N$ - $I$ - $S$  junction. At a larger voltage, the usual Joule heating is recovered, and electrons are heated above the thermal bath temperature.

The cooling and heating of the source electronic bath is illustrated for sample B in Fig. 2, left. Here one  $N$ - $I$ - $S$  junction to the source is used for thermometry, while a second junction acts as a cooler used for cooling and heating. At a low cooler bias  $V_{\text{cool}}$ , the electronic temperature  $T_e$  is below the bath temperature  $T_b$  of 152 mK (indicated by a horizontal dashed line in Fig. 2, left) so that cooling is achieved. The maximum temperature reduction of about 50 mK is reached at a potential drop  $V_{\text{cool}}$  of about 190  $\mu\text{eV}$ , close to the gap  $\Delta$  for Al. A larger cooling is obtained when the gate potential is adjusted so that electron

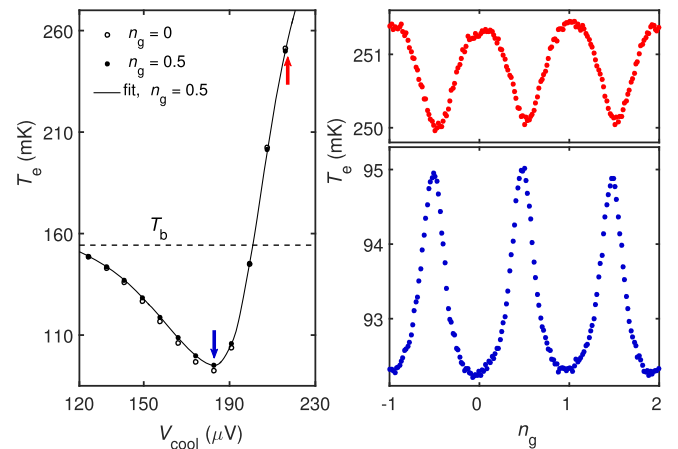


FIG. 2. Left: Variation of electronic temperature  $T_e$  of the sample B source with cooler bias voltage, at gate open ( $n_g = 0.5$ ) and gate closed ( $n_g = 0$ ) states, at a bath temperature  $T_b$  of 152 mK. The full line is a fit of the gate-open state data; see the text. Right: Temperature modulation by the gate voltage expressed in terms of induced charge  $n_g$  in the heating regime (top) and in the cooling regime (bottom) at cooler bias points indicated by the blue and red arrows in the left plot.

transport through the SET is blocked ( $n_g = 0$ ) and so is thermal transport through it. At a higher bias of the cooler ( $V_{\text{cool}} > \Delta$ ), an electron overheating is obtained:  $T_e > T_b$ . Again, the electron temperature change (here an increase) is larger when the SET is blocked. The electron temperature at a fixed cooler bias but as a function of the gate potential is displayed in Fig. 2, right. Clear temperature oscillations are obtained, with an opposite sign for the electron cooling and the overheating regimes. This demonstrates the contribution of the thermal conductance of the SET to heat transport.

In order to quantify the thermal conductance through the SET, we describe the thermal balance in the source following a thermal model depicted in Fig. 1(b). In this model, the electron bath in the source receives the power  $\dot{Q}_{\text{cool}}$  from the cooler junction, with a positive or negative sign corresponding to cooling or heating, respectively. It can be calculated from [32]  $\dot{Q}_{\text{cool}} = (1/e^2 R_{\text{cool}}) \int_{-\infty}^{\infty} (E - eV_{\text{cool}}) n_S(E) [f_{\text{source}}(E - eV_{\text{cool}}) - f_S(E)] dE - \dot{Q}_0$ , where  $R_{\text{cool}}$  is the tunnel junction resistance of the cooler,  $n_S(E)$  is the (BCS) density of states of the superconductor, and  $f_{\text{source},S}(E)$  is the thermal energy distribution function in the source or the  $S$  lead of the cooler at respective temperatures  $T_e$  and  $T_S$ . The parasitic power  $\dot{Q}_0$  takes into account imperfect thermalization of the electrical connections. The main energy relaxation channel for the source electrons is the coupling to phonons, with a power following  $\dot{Q}_{e\text{-ph}} = \Sigma \mathcal{V} (T_e^5 - T_{\text{ph}}^5)$ , where  $\Sigma$  is characteristic of the material,  $\mathcal{V}$  is the volume, and  $T_{\text{ph}}$  is the phonon temperature here assumed to be equal to the bath temperature [32]. Eventually, the SET transmits a power  $\dot{Q}_{\text{SET}}$  to the source.

Let us first consider the gate-open position  $n_g = 0.5$ , where the two charge states involved in electron transport have the same electrostatic energy. Electron transport is thus (for small barrier transparency) unaffected by electron interaction, and the Wiedemann-Franz law is expected to be valid. This is confirmed by numerical calculations at  $k_B T \ll E_C$  [19]. The power  $\dot{Q}_{\text{SET}}$  can thus be calculated from the measured differential conductance for charge  $dI/dV$  at a low bias. We use the thermal balance for the source electrons  $\dot{Q}_{\text{SET}} - \dot{Q}_{\text{cool}} - \dot{Q}_{e\text{-ph}} = 0$  to extract the cooling or heating power  $\dot{Q}_{\text{cool}}$ . Here the electron-phonon coupling power  $\dot{Q}_{e\text{-ph}}$  is calculated using the actual volume  $\mathcal{V}$  and a parameter value:  $\Sigma = 2.8 \text{ nW } \mu\text{m}^3 \text{ K}^{-5}$ , close to the expected value for Cu [32]. The parasitic power  $\dot{Q}_0$  is found to be 0.1 fW in agreement with previous works [8]. From the values of  $\dot{Q}_{\text{cool}}$  and taking into account the measured electronic temperature, the imposed cooler voltage, and the Al energy gap, one extracts the superconducting lead temperature as a function of the bias  $V_{\text{cool}}$  of the cooler. Values, obtained for this temperature  $T_S$ , up to 450 mK [21] are in line with expectations in a device where no specific care was put for proper quasiparticle evacuation [35].

The preceding analysis at the gate-open state provides us with a full knowledge of the thermal behavior of the source, including all physical parameters for electronic cooling and electron-phonon coupling. We now assume that, whatever the gate potential is, the temperature of the superconducting leads of the cooler varies with the cooler's bias as determined above in the gate-open case. The measured values of the source electronic temperature  $T_e(n_g)$  are used to calculate the power flowing through the SET as  $\dot{Q}_{\text{SET}} = \dot{Q}_{\text{cool}} + \dot{Q}_{e\text{-ph}}$  as a function of  $n_g$ . Considering the limit of a small temperature difference, the SET heat conductance is then calculated as  $\kappa = \dot{Q}_{\text{SET}} / (T_b - T_e)$ .

Figure 3 shows both the heat conductance  $\kappa$  and the charge conductance  $\sigma$  for samples A and B, as a function of the gate potential. Both quantities were measured at the same bath temperature. An SET bias of about 20  $\mu\text{V}$  and an electron cooling by about 25 mK were used for the charge and the heat transport measurements, respectively. The charge conductance is plotted in units of the low-bias gate-open conductance  $\sigma_0$ . The heat conductance is plotted in units of the Wiedemann-Franz value in the gate-open state  $\kappa_0 = \sigma_0 L_0 T_m(n_g = 0.5)$ . We use here the mean temperature  $T_m = (T_e + T_b)/2$  so that a linear response is

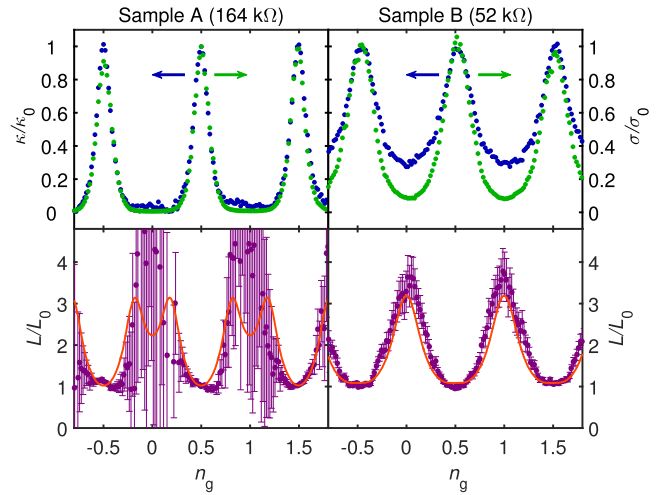


FIG. 3. Top: Thermal (blue dots) and charge (green dots) conductances of the SET at a bath temperature of 132 (left, sample A) and 152 mK (right, sample B) in units of the conductances in the gate-open state  $\kappa_0$  and  $\sigma_0$ . The thermal flow through the SET was calculated assuming that the Wiedemann-Franz law is fulfilled at the gate-open state. The charge transport was measured at a bias of 22.4 (sample A) and 19.2  $\mu\text{V}$  (sample B). The heat transport data were acquired by cooling the source electronic bath by 30 (sample A) and 22 mK (sample B) below the bath temperature. Bottom: Lorenz ratio (purple dots) defined as  $L/L_0$ , where  $L = \kappa / (\sigma T_m)$  for sample A (left) and sample B (right). The error bars are related to the uncertainty in the temperature measurement. The Wiedemann-Franz law sets  $L = L_0$ . The red line is the theoretical prediction based on Ref. [19].

expected in the Wiedemann-Franz regime even for the case of a significant temperature difference  $T_e - T_b$  [21].

For both samples *A* and *B*, the charge and heat conductances oscillate with  $n_g$ . In the case of sample *A* (top left), the two conductances mostly overlap over the full gate potential range. Close to the gate-closed state, the two conductances seem to deviate one from the other, but their absolute values are small. In contrast, sample *B* exhibits a clear deviation from the Wiedemann-Franz law. At the gate-closed state, the heat conductance clearly exceeds the charge conductance multiplied by  $L_0 T$ .

In order to get more insight, let us now consider the Lorenz factor defined as  $L/L_0$  with  $L = \kappa/(\sigma T_m)$ . The Wiedemann-Franz law sets a Lorenz factor equal to unity. In contrast, for sample *B* the Lorenz factor (Fig. 3, bottom right) oscillates between 1 at the gate-open state and about 4 at the gate-closed state. This is the main result of this work. Sample *A* shows essentially the same behavior over the gate potential range where it can be accurately determined, whereas error bars are very large in the vicinity of the gate-closed state due to vanishingly small conductances. We obtained similar results for the whole range of bias points of the cooler, in both the cooling and the heating regimes [21].

The physical origin of the violation of the Wiedemann-Franz law resides in the energy selectivity of electron transport through an SET [36]. As a consequence of this, the population of electrons flowing through the SET is nonthermal. For instance, at the gate-closed state, only electrons with an energy (counted from the Fermi level) above the charging energy  $E_C$  contribute to the zero-bias SET conductance. These electrons obviously carry the same (electron) charge but a higher energy. Thus, the heat conductance does not decay due to interactions as much as the charge conductance does, and the Lorenz number exceeds its basic value  $L_0$ . Electron cotunneling can counterbalance this, as it involves electrons with an energy close to the Fermi level. The crossover to the cotunneling regime shows up at the gate-closed state as a maximum of the Lorenz factor at a temperature  $T \approx 0.1E_C/k_B$  [19].

We have calculated the theoretical Lorenz factor for our samples using the theory of Ref. [19]. Figure 3, bottom, shows as full lines the calculated Lorenz factor in parallel with the experimental data. As for parameters, we used the measured values of the SET conductance and average temperature as well as  $k_B T/E_C = 0.06$  and  $0.12$  for sample *A* and *B*, respectively. The latter values are close to the calculated ones  $0.067$  and  $0.122$ , respectively. The theoretical prediction and the experimental data match very well, within error bars. For sample *A*, the calculated Lorenz number shows a relative minimum in the gate-closed state, which cannot be checked in the experiment due to experimental uncertainties.

Furthermore, we investigated the power  $\dot{Q}_{\text{SET}}$  flowing through the SET beyond the regime of small temperature differences. In the linear regime, the thermal conductance  $\kappa$  is proportional to the temperature, leading to the quadratic

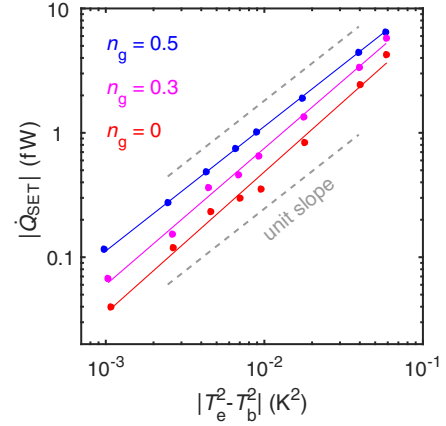


FIG. 4. Nonlinear heat flow through the sample *B* SET at different gate states as a function of the difference of the squared temperatures between the source and the bath (symbols) together with power-law fits (full lines). The slopes are 1.00, 1.10, and 1.14, respectively, at gate positions  $n_g = 0.5, 0.3,$  and  $0$ . The unit slope expected for the linear regime of heat transport is shown as dotted gray lines.

dependence of the heat power on the source ( $T_e$ ) and drain ( $T_b$ ) temperatures:  $\dot{Q}_{\text{SET}} \propto T_b^2 - T_e^2$  [21]. Figure 4 compares experimental data (dots) covering both the cooling and the heating regimes to the latter law, on a log-log plot. In the gate-open case  $n_g = 0.5$ , the slope is 1 as assumed in the calibration. Away from the gate-open state, a larger slope is obtained, up to 1.14 at  $n_g = 0$ . Further theoretical work is needed to compare this observation to theoretical predictions.

In conclusion, we have demonstrated that the heat transport through an SET can be driven by a gate potential, making the SET a heat switch. The celebrated Wiedemann-Franz law is strongly violated away from the charge degeneracy positions. Our experimental data agree very well with theoretical predictions. As a prospect, investigating SETs where the island is a quantum dot could exhibit new thermoelectric effects driven by a single energy level [37,38].

We acknowledge financial support from the Academy of Finland (Projects No. 272218, No. 284594, and No. 275167) and from the Nanosciences Foundation, Nanosciences Foundation, under the auspices of the Université Grenoble Alpes Foundation. We acknowledge the availability of the facilities and technical support by Otaniemi research infrastructure for Micro and Nanotechnologies (OtaNano). We are indebted to the late F. W. J. Hekking for many illuminating discussions on the topic.

B. D. and J. T. P. contributed equally to this work.

- [1] B. Sothmann, R. Sanchez, and A. N. Jordan, Thermoelectric energy harvesting with quantum dots, *Nanotechnology* **26**, 032001 (2015).

- [2] Y. Dubi and M. Di Ventra, Colloquium: Heat flow and thermoelectricity in atomic and molecular junctions, *Rev. Mod. Phys.* **83**, 131 (2011).
- [3] O. Chiatti, J. Nicholls, Y. Proskuryakov, N. Lumpkin, I. Farrer, and D. Ritchie, Quantum Thermal Conductance of Electrons in a One-Dimensional Wire, *Phys. Rev. Lett.* **97**, 056601 (2006).
- [4] M. Banerjee, M. Heiblum, A. Rosenblatt, Y. Oreg, D. E. Feldman, A. Stern, and V. Umansky, Observed quantization of anyonic heat flow, *Nature (London)* **545**, 75 (2017).
- [5] L. Cui, W. Jeong, S. Hur, M. Matt, J. C. Klockner, F. Pauly, P. Nielaba, J. Carlos Cuevas, E. Meyhofer, and P. Reddy, Quantized thermal transport in single-atom junctions, *Science* **355**, 1192 (2017).
- [6] N. Mosso, U. Drechsler, F. Menges, P. Nirmalraj, S. Karg, H. Riel, and B. Gotsmann, Heat transport through atomic contacts, *Nat. Nanotechnol.* **12**, 430 (2017).
- [7] K. Schwab and M. L. Roukes, Measurement of the quantum of thermal conductance, *Nature (London)* **404**, 974 (2000).
- [8] M. Meschke, W. Guichard, and J. P. Pekola, Single-mode heat conduction by photons, *Nature (London)* **444**, 187 (2006).
- [9] L. W. Molenkamp, Th. Gravier, H. van Houten, O. J. A. Buijk, M. A. A. Mabeoone, and C. T. Foxon, Peltier Coefficient and Thermal Conductance of a Quantum Point Contact, *Phys. Rev. Lett.* **68**, 3765 (1992).
- [10] E. A. Hoffmann, H. A. Nilsson, J. E. Matthews, N. Nakpathomkun, A. I. Persson, L. Samuelson, and H. Linke, Measuring temperature gradients over nanometer length scales, *Nano Lett.* **9**, 779 (2009).
- [11] S. Jézouin, F. D. Parmentier, A. Anthore, U. Gennser, A. Cavanna, Y. Jin, and F. Pierre, Quantum limit of heat flow across a single electronic channel, *Science* **342**, 601 (2013).
- [12] D. V. Averin and K. K. Likharev, Coulomb blockade of single-electron tunneling, and coherent oscillations in small tunnel junctions, *J. Low Temp. Phys.* **62**, 345 (1986).
- [13] C. W. J. Beenakker and A. A. M. Staring, Theory of the thermopower of a quantum dot, *Phys. Rev. B* **46**, 9667 (1992).
- [14] D. Boese and R. Fazio, Thermoelectric effects in Kondo correlated quantum dots, theory of the thermopower of a quantum dot, *Europhys. Lett.* **56**, 576 (2001).
- [15] M. Turek and K. A. Matveev, Cotunneling thermopower of single electron transistors, *Phys. Rev. B* **65**, 115332 (2002).
- [16] B. Kubala and J. König, Quantum-fluctuation effects on the thermopower of a single-electron transistor, *Phys. Rev. B* **73**, 195316 (2006).
- [17] M. Tsaousidou and G. P. Triberis, Thermal conductance of a weakly coupled quantum dot, *AIP Conf. Proc.* **893**, 801 (2007).
- [18] X. Zianni, Coulomb oscillations in the electron thermal conductance of a dot in the linear regime, *Phys. Rev. B* **75**, 045344 (2007).
- [19] B. Kubala, J. König, and J. Pekola, Violation of the Wiedemann-Franz Law in a Single-Electron Transistor, *Phys. Rev. Lett.* **100**, 066801 (2008).
- [20] Ya. I. Rodionov, I. S. Burmistrov, and N. M. Chitchev, Relaxation dynamics of the electron distribution in the Coulomb-blockade problem, *Phys. Rev. B* **82**, 155317 (2010).
- [21] See Supplemental Material at <http://link.aps.org/supplemental/10.1103/PhysRevLett.119.077701> for details on sample design, fabrication and characterization, and a discussion of the heat balance analysis, as well as additional experimental material, which contains Refs. [22–29].
- [22] J. T. Peltonen, V. F. Maisi, S. Singh, E. Mannila, and J. P. Pekola, On-chip error counting for hybrid metallic single-electron turnstiles, [arXiv:1512.00374](https://arxiv.org/abs/1512.00374).
- [23] J. P. Pekola, V. F. Maisi, S. Kafanov, N. Chekurov, A. Kempinen, Yu. A. Pashkin, O.-P. Saira, M. Möttönen, and J. S. Tsai, Photon-Assisted Tunneling as an Origin of the Dynes Density of States, *Phys. Rev. Lett.* **105**, 026803 (2010).
- [24] S. Rajauria, P. S. Luo, T. Fournier, F. W. J. Hekking, H. Courtois, and B. Pannetier, Electron and Phonon Cooling in a Superconductor-Normal Metal-Superconductor Tunnel Junction, *Phys. Rev. Lett.* **99**, 047004 (2007).
- [25] J. T. Peltonen, P. Virtanen, M. Meschke, J. V. Koski, T. T. Heikkilä, and J. P. Pekola, Thermal Conductance by the Inverse Proximity Effect in a Superconductor, *Phys. Rev. Lett.* **105**, 097004 (2010).
- [26] G. L. Ingold and Yu. V. Nazarov, in *Single Charge Tunneling*, edited by H. Grabert and M. H. Devoret, NATO ASI Ser. B Vol. 294 (Plenum, New York, 1992), p. 21107.
- [27] K. L. Viisanen and J. P. Pekola, Anomalous electronic heat capacity of copper nanowires at sub-kelvin temperatures, [arXiv:1606.02985](https://arxiv.org/abs/1606.02985).
- [28] H. S. Knowles, V. F. Maisi, and J. P. Pekola, Probing quasiparticle excitations in a hybrid single electron transistor, *Appl. Phys. Lett.* **100**, 262601 (2012).
- [29] S. Rajauria, L. M. A. Pascal, Ph. Gandit, F. W. J. Hekking, B. Pannetier, and H. Courtois, Efficiency of quasiparticle evacuation in superconducting devices, *Phys. Rev. B* **85**, 020505(R) (2012).
- [30] J. V. Koski, J. T. Peltonen, M. Meschke, and J. P. Pekola, Laterally proximized aluminum tunnel junctions, *Appl. Phys. Lett.* **98**, 203501 (2011).
- [31] H. Pothier, S. Guéron, N. O. Birge, D. Estève, and M. H. Devoret, Energy Distribution Function of Quasiparticles in Mesoscopic Wires, *Phys. Rev. Lett.* **79**, 3490 (1997).
- [32] F. Giazotto, T. T. Heikkilä, A. Luukanen, A. M. Savin, and J. P. Pekola, Opportunities for mesoscopics in thermometry and refrigeration: Physics and applications, *Rev. Mod. Phys.* **78**, 217 (2006).
- [33] M. Nahum and J. M. Martinis, Ultrasensitive hot-electron microbolometer, *Appl. Phys. Lett.* **63**, 3075 (1993).
- [34] M. Nahum, T. M. Eiles, and J. M. Martinis, Electronic micro-refrigerator based on a normal-insulator-superconductor tunnel junction, *Appl. Phys. Lett.* **65**, 3123 (1994).
- [35] H. Q. Nguyen, T. Aref, V. J. Kaupilla, M. Meschke, C. B. Winkelmann, H. Courtois, and J. P. Pekola, Trapping hot quasi-particles in a high-power superconducting electronic cooler, *New J. Phys.* **15**, 085013 (2013).
- [36] C. Altimiras, H. le Sueur, U. Gennser, A. Anthore, A. Cavanna, D. Mailly, and F. Pierre, Chargeless Heat Transport in the Fractional Quantum Hall Regime, *Phys. Rev. Lett.* **109**, 026803 (2012).
- [37] D. M. T. van Zanten, D. M. Basko, I. M. Khaymovich, J. P. Pekola, H. Courtois, and C. B. Winkelmann, Single Quantum Level Electron Turnstile, *Phys. Rev. Lett.* **116**, 166801 (2016).
- [38] R. Scheibner, H. Buhmann, D. Reuter, M. N. Kiselev, and L. W. Molenkamp, Thermopower of a Kondo Spin-Correlated Quantum Dot, *Phys. Rev. Lett.* **95**, 176602 (2005).